PHYSICAL REVIEW B **79**, 155202 (2009)

Nonsubstitutional single-atom defects in the $Ge_{1-x}Sn_x$ alloy

C. I. Ventura,[1] J. D. Fuhr,[1] and R. A. Barrio[2]
[1]*Centro Atómico Bariloche, 8400-Bariloche, Argentina*
[2]*Instituto de Física, U.N.A.M., 01000-Mexico D.F., Mexico*

(Received 30 July 2008; revised manuscript received 30 January 2009; published 3 April 2009)

$Ge_{1-x}Sn_x$ alloys have proved difficult to form at large x, contrary to what happens with other group IV semiconductor combinations. However, at low x they are typical examples of well-behaved substitutional compounds, which is desirable for harnessing the electronic properties of narrow-band semiconductors. In this paper, we propose the appearance of another kind of single-site defect (β-Sn), consisting of a single Sn atom in the center of a Ge divacancy, that may account for these facts. Accordingly, we examine the electronic and structural properties of these alloys by performing extensive numerical *ab initio* calculations around local defects. The results show that the environment of the β defect relaxes toward a cubic octahedral configuration, facilitating the nucleation of metallic white tin and its segregation, as found in amorphous samples. Using the information stemming from these local defect calculations, we built a simple statistical model to investigate at which concentration these β defects can be formed in thermal equilibrium. These results agree remarkably well with experimental findings, concerning the critical concentration above which the homogeneous alloys cannot be formed at room temperature. Our model also predicts the observed fact that at lower temperature the critical concentration increases. We also performed single-site effective-field calculations of the electronic structure.

DOI: 10.1103/PhysRevB.79.155202 PACS number(s): 71.20.Nr, 71.55.Ak, 71.15.−m

I. INTRODUCTION

The search for direct energy-gap materials based on group IV semiconductors is not new,[1–4] but has been hindered for a long time by sample preparation problems. The importance of such compounds due to their potential for technological applications was recognized early. A low-energy direct gap would enable the use for infrared applications, long-wavelength photodetector sand emitters, LED, and infrared laser applications, i.e., in general allow the use for optoelectronic devices. Combined with the use of group IV elements, this would be ideal for compatibility and integration with the Si-based technology.

While Ge is an indirect-gap semiconductor (at room temperature it has a 0.66 eV indirect gap and 0.81 eV is the direct band gap at the Γ symmetry point of the fcc diamond Brillouin zone),[5] gray tin (α-Sn) is a semimetal with the same tetrahedral crystal structure (also often labeled as a zero-gap semiconductor, due to the overlap at the zone center of its valence and conduction bands, by about 0.42 eV).[6] It was recognized that $Ge_{1-x}Sn_x$ alloys should provide tunable gap materials, controlled by concentration,[7–9] and a route for obtaining direct-gap group IV systems compatible with Si integrated circuits. The first experiments providing evidence for the indirect-to-direct-gap transition date from 1997,[9] while only recently crystalline samples of the quality and stability required by device applications were prepared.[10–12] In the last two years further important uses for these materials were proposed: they were studied[13] in connection with their potential use for nanostructured thermoelectric cooling devices, and the higher electron and hole mobilities which might be reached by alloying and straining.[14] Thus, they might allow to overcome current integrated circuit limitations to develop higher speed Si microelectronics.

The electronic structures of most semiconductor alloys are smooth functions of their composition, thus providing a versatile tool for device engineering. Alloys of elemental semiconductors such as group IV elements Si and Ge, and alloys of III–V compounds as GaAs, AlAs, InAs, and InP play key roles in microelectronics and optoelectronics. $Si_{1-x}Ge_x$ is nearly ideal as it has lattice constant and interband optical transition energies which are essentially linear in x. However, Si-based photodetectors, e.g., cannot cover the optical communication wavelength windows (1310–1550 nm). Pure Ge barely reaches the 1550 nm range, but it does not grow well on Si substrates: this was solved by alloying Ge with Sn. Even 2% Sn achieves an order of magnitude increase in absorption at 1550 nm, and the alloy grows with device quality on Si substrates.[10,11,15,16]

Binary alloys of group IV semiconductors are usually easy to prepare at any concentration, but this is not the case for the $Ge_{1-x}Sn_x$ alloy. Homogeneous alloys have proved difficult to form at large x. This has considerably reduced its applicability in the fabrication of electronic devices. Other group IV alloys are formed by simple substitution of one component by the other, maintaining the overall tetrahedral environment of the diamond lattice. This is true even in amorphous alloys.

At the low concentrations at which it has been possible to prepare homogeneous $Ge_{1-x}Sn_x$ alloys,[10] it has been found that Sn occupies substitutional sites. This results in a smooth dependence of its electronic properties as a function of concentration, which is desirable to tailor key quantities as the band gap and the density of states at the Fermi level. However, at Sn concentrations higher than 20% this picture breaks down because Sn exhibits the tendency to segregate in the cubic β phase, which is metallic. This spoils the semiconducting properties.

The main point of interest of our present work is to try to understand theoretically the structural and dynamical mechanisms that trigger this peculiar segregation. Some authors[10] attribute this to the large difference in size between Ge and Sn atoms and to the large lattice mismatch. This cannot be the whole picture, because segregation has also been observed to begin at the same concentrations in amorphous alloys.[17]

Our hypothesis is that the difficulty in the formation of homogeneous alloys can be explained by the nucleation of the metastable β-Sn phase ("white tin," which is a metal and cubic) in the perfect tetrahedral lattice of the alloy.

We shall investigate the mechanisms by which clusters of few Sn atoms can acquire a cubic symmetry in the tetrahedral Ge matrix. Accordingly, we assume that there exists a defect with a single Sn atom bonded to six neighboring Ge atoms. This is possible due to the important role of the d orbitals in the electronic structure of both atoms. The existence of such a defect in amorphous Ge-Sn alloys has already been confirmed by detailed Mössbauer experiments,[17] which in fact show a signal corresponding to a Sn atom in an octahedral environment, besides the expected signal of the substitutional tetrahedral α-Sn defect. Furthermore, signatures of the presence of two sites for the Sn atoms were also found with ^{119}Sn Mössbauer spectroscopy in nanoscale mixtures of Ge/Sn.[18] This point defect, which we shall call β-Sn defect from now on, can be envisaged as a single Sn atom at the center of a Ge divacancy. This defect (although rare) should produce a large negative (shrinking) elastic field around it, opposite to the usual positive (expansive) elastic field of the α-Sn defect, due to the larger size of Sn as compared to Ge.

In the following section we will present our hypothesis for the incorporation of Sn in the Ge lattice in more detail, in Sec. III we will describe the different approaches which we have used to tackle diverse aspects of the problem systematically as well as the main results obtained with each, and their implications. In particular, the simple statistical model we proposed to study the formation of $Ge_{1-x}Sn_x$ alloys, based on information obtained through our *ab initio* local defect study and the experimental fact that β-Sn defects have already been found in nonhomogeneous samples, provide a quite complete scenario and consistent explanation for the experimental difficulties in the formation of homogeneous alloys. Finally, we present our conclusions and discuss how our results might be useful to solve problems for sample preparation with device quality, as required for the important technological applications envisaged for these alloys, and give an outlook to further interesting research on these materials.

II. HYPOTHESIS: MECHANISMS FOR Sn INCORPORATION IN THE Ge LATTICE

The proposed mechanism goes as follows: small amounts of Sn incorporate very easily in isolated places in the Ge matrix as α defects. The strain caused by the size mismatch increases with the concentration of these defects (x_α), causing a propitious environment for the formation of the β defect, since that would release the strain in the lattice. As the α defects get closer to the existing β defects they attract each other through their elastic fields, and if they merge, further elastic energy would be released and the small clusters of Sn atoms would relax to a cubic symmetry. Therefore, if diffusion allows the migration of defects during the formation, the material would present a natural tendency to segregate the Sn clusters to its surface, in order to attain equilibrium.

All these ideas have to be tested either by numerical calculations or statistical models. First of all, one needs accurate *ab initio* electronic calculations to estimate the scale of energies involved in the immediate environment around each defect. These calculations also provide the relaxed configurations of the defects, allowing one to test the cubic symmetry locally. Furthermore, one can use the dependence of the electronic energy with the volume to estimate a pressure directly related to the elastic field caused by the defects on their local environment. All these quantities allow to construct a model for the behavior of the macroscopic system, which is needed to test if one can form β defects in the alloy, and at which concentrations they would appear.

The electronic properties of the homogeneous alloy can be tested by performing effective-field calculations, such as the virtual-crystal approximation (VCA) (Ref. 19) or the coherent-potential approximation (CPA).[20] These approximations are known to give excellent predictions in many substitutional semiconductor alloys.[21,22] Since CPA electronic structure results were lacking we decided to undertake them to complete the information available for these alloys. In Sec. III C 3 we present our results and discuss their implications.

In Sec. III we present in detail these three approaches to the problem, and discuss the results in terms of the main hypothesis presented here.

III. NUMERICAL AND MEAN FIELD STUDIES

A. Local defect electronic calculations

A good starting point to examine the properties of local defects in an alloy is to perform *ab initio* electronic calculations using the common techniques of density-functional theory.

We have basically two different point defects to be studied: (1) a Sn atom sitting substitutionally in a perfect Ge diamond lattice, and (2) a single Sn atom in a cage of six Ge atoms that surround a double vacancy in the perfect diamond lattice. This cage has a long axis along the (111) direction, but it is not clear if the presence of the impurity inside the cage should modify this symmetry.

The electronic energies depend on the local environment around the defect and the respective relaxation of the lattice, which involves changes in lattice parameter (or cell volume) and in the individual cell-atom positions. We have considered unit cells of different sizes around the point defect in order to address these issues.

On one hand, we analyzed to what degree the energies and the lattice relaxation around the defect depend on the size of the cell, and through this we discussed the elastic field caused by the defect. On the other hand, we studied more complex defect environments involving several Sn impurities. We have considered unit cells of 8 atoms, as the ones studied in previous works,[9,23] as well as some larger cells, with 16 and 64 atoms, designed to better assess the preferred configurations when multiple defects are present.

TABLE I. Results of electronic calculations using WIEN-2K code (L/APW+lo with GGA) for the cells with configurations described in the text. Successive columns report: corresponding “alloy concentration” (x); lattice parameter (a) of fully relaxed crystal structure; cohesive energy (E_c) (relative to bulk Ge and Sn); cohesive energy per cell atom: fully relaxed local defect energy (E_d); pressure (P) due to defect; and partially relaxed cohesive energy ($E_c^{V_{\mathrm{Ge}}}$) and local defect energy ($E_d^{V_{\mathrm{Ge}}}$) per cell atom: at Ge cell volume. All energies given in eV.

Cell	x	a (Å)	E_c	E_d	P (GPa)	$E_c^{V_{\mathrm{Ge}}}$	$E_d^{V_{\mathrm{Ge}}}$
Ge2	0	5.77	0	0	0	0	0
Sn2	1	6.65	0	0			
Ge7Sn1	0.125	5.88	0.237	0.030	3.79	0.371	0.046
Ge6Sn1$_\beta$	0.143	5.58	1.791	0.256	−3.43	2.007	0.287
Ge6Sn2$_\parallel$	0.25	6.00	0.415	0.052	7.99	0.954	0.119
Ge15Sn1	0.062	5.82	0.287	0.018	1.81	0.360	0.022
Ge14Sn1$_\beta$	0.066	5.72	1.804	0.120	−0.98	1.832	0.122
Ge14Sn2$_\parallel$	0.125	5.89	0.652	0.041	3.99	0.944	0.059
Ge14Sn2	0.125	5.90	0.462	0.029	3.86	0.730	0.046
Ge12Sn2$_{2\beta}$	0.143	5.89	3.584	0.256	−3.42	4.022	0.287
Ge11Sn5	0.31	6.10	1.221	0.076	11.01	3.083	0.193
Ge11Sn4$_a$	0.26	5.85	1.330	0.089	1.85	1.419	0.095
Ge11Sn4$_b$	0.26	5.84	1.333	0.089	1.85	1.431	0.095
Ge64	0	5.76	0	0	0	0	0
Sn64	1	6.63	0	0			
Ge56Sn6	0.097	5.77	2.624	0.042	0.47	6.973	0.112
Ge56Sn7$_{\beta'}$	0.111	5.81	1.860	0.030	1.71	2.093	0.033
GeSn	0.5	6.21	0.052	0.026	17.93	0.594	0.297

We have determined the defect energies per atom, relative to the pure Ge and Sn cohesive energy reference values, allowing *full relaxation* of the different cells studied with respect to the Ge lattice (i.e., allowing changes in lattice parameter and of individual positions of the atoms in the cell). Specifically, for a unit cell consisting of n Ge atoms and m Sn atoms, we define the energy of the defect (E_d) as the cohesive energy per atom,

$$E_d = \frac{E_{\mathrm{Cell}(\mathrm{Ge}_n\mathrm{Sn}_m)} - nE_{\mathrm{Ge\text{-}bulk}} - mE_{\mathrm{Sn\text{-}bulk,}}}{n+m}, \tag{1}$$

where $E_{\mathrm{Cell}(\mathrm{Ge}_n\mathrm{Sn}_m)}$ is the total energy of the fully relaxed cell with the defect, and the denominator is the total number of atoms in the cell. $E_{\mathrm{Ge\text{-}bulk}}$ and $E_{\mathrm{Sn\text{-}bulk}}$ are the bulk Ge and Sn cohesive energies per atom, corresponding to perfect diamond lattices of Ge and gray tin (α-Sn). We have also calculated the *partially relaxed* local defect energies ($E_d^{V_{\mathrm{Ge}}}$) per cell atom: fixing the cell volume at the value V_{Ge} corresponding to bulk Ge, allowing only relaxation of the positions of the individual atoms inside the cell.

In order to discuss the elastic field caused by the presence of the defect, we also determined the pressure exerted by each type of local defect on the unit cell. This is obtained from the dependence of the total energy with the volume (i.e., using partially relaxed energies at fixed cell volume E^{V}). We define the pressure as

$$P = -\left.\frac{\partial E^V}{\partial V}\right|_{V=V_{\mathrm{Ge}}}, \tag{2}$$

calculated at the unit-cell volume which corresponds to bulk Ge. In our convention, a positive pressure P will mean that expansion of the lattice with respect to bulk Ge is favored.

The numerical calculations were done using the full-potential linearized augmented plane wave plus local-orbital (L/APW+lo) method, as implemented in the WIEN2K code.[24–26] The exchange-correlation effects were treated within the generalized gradient approximation (GGA) using the Perdew-Burke-Ernzerhof form.[27] The radii of the muffin-tin spheres (R_{MT}) were chosen to be 2.25 bohr for both Ge and Sn atoms. The cutoff parameter $R_{\mathrm{MT}}-K_{\mathrm{max}}$ for limiting the number of the plane waves was set equal to 8, with $K_{\mathrm{max}}(=8/2.25=3.55\ \mathrm{bohr}^{-1})$ the largest reciprocal-lattice vector used in the plane-wave expansion. To integrate inside the Brillouin zone (BZ) we used a k sampling with $(7\times 7\times 7)$, $(6\times 6\times 6)$, and $(4\times 4\times 4)$ Monkhorst-Pack[28] meshes, for unit cells with 8, 16, and 64 atoms, respectively. In all cases, all atoms in the unit cell were allowed to fully relax independently and, except otherwise stated, also lattice parameter (i.e., cell volume) relaxation was allowed. In Table I we summarize the results of our *ab initio* electronic structure calculations. The first column identifies each of the local configurations considered. We have labeled the unit cells by explicitly indicating the number of atoms of each species they contain, further details will be given below.

First, we have considered the two limiting cases of the alloy, namely, the perfect diamond lattices of Ge and gray tin, in order to extract their cohesive energies as reference values for the local defects. In these cases (labeled as Ge2 and Sn2 in Table I), we used the Wigner-Seitz cells for diamond, containing two atoms and periodic boundary conditions. We also calculated the corresponding bulk energies and lattice parameters for cells including 64 atoms: Ge64 and Sn64, resulting in cohesive energies differing from the two-atom cell values by less than 0.1 meV. Observe in the table that also the lattice parameter changes are negligible.

In the 8-atom cells we studied a single substitutional α-Sn defect (the Ge/Sn1 case of Table I), a nonsubstitutional β-Sn defect with a Sn atom at the center of a divacancy in the Ge lattice (case Ge6Sn1_β), and the pair defect consisting of two contiguous α defects in which the two Sn atoms align parallel to the (111) symmetry axis of the diamond lattice (case Ge6Sn$2_\parallel$). In the latter case, we have verified that starting from different orientations of the pair of Sn atoms, this symmetry is the one corresponding to the minimum of the total relaxation process. These 8-atom configurations were studied before, within the local-density approximation (LDA).[9] In agreement with the well-known general trends, the GGA yields slightly lower cohesion energies and larger lattice parameters than LDA, in the cases where we can compare our results with previous LDA calculations.[8,9]

We also studied the single α-Sn defect and the pair defect configurations in a 16-atom cell to see the effect of the size of the cell on the relaxed configurations. In particular, the fact that the energy obtained for two independent (noncontiguous) α-Sn defects in a 16-site cell (Ge14Sn2) is approximately twice the energy of one α defect in the 8-site cell (Ge7Sn1) is a further indication that our results are reasonably size independent. This is also confirmed by analyzing the case for β defects, where it is also evident by comparison of the cases Ge6Sn1_β and Ge12Sn$2_{2\beta}$.

The trend with cell volume and defect concentration exhibited by the data contained in Table I is the expected one. When one compares the same defect for two different defect concentrations (for example one α defect in the 8-atom and in the 16-atom cells), one must consider two contributions to the cohesive energy difference:

(i) At fixed lattice parameter, the interaction between neighbor defects in the lattice is larger for the smaller unit-cell case due to less available degree of freedom for the partial relaxation, resulting in a higher cohesive energy, as evident in the ($E_c^{V_{\mathrm{Ge}}}$) tabulated. For example the cohesive energy of one α defect in the 8-atom cell is 0.011 eV higher than for one α defect in the 16-atom case.

(ii) The second ingredient is the energy gained by volume relaxation, which from simple considerations can be seen to be approximately proportional to $1/V$. For example, the energy gained by volume relaxation of one α defect in the 8-atom cell (0.134 eV) is close to double of that gained for the same defect in the 16-atom cell (0.073 eV). Thus, volume relaxation has an important effect here resulting in an overall lower totally relaxed cohesive energy (E_c) for the smaller unit cell (higher concentration case).

If one now analyzes the trend of the above defined pressure [Eq. (2)] with cell size, one observes that it also has a $1/V$ dependence for large unit cells. If one rescaled the pressure with a factor equal to V_{Ge}, the obtained value for each given defect would go to a constant at large unit-cell volumes. In particular, for the single α defect the rescaled pressure now yields a very small difference between the values obtained for the 8- and 16-atom unit cells. This shows that the 8-atom unit cell is already allowing almost full local relaxation around this defect, thus exhibiting the local nature of the pressure it exerts. The result is also consistent with the small difference in the α defect energy between the two unit cells at the same volume ($E_c^{V_{\mathrm{Ge}}}$). Meanwhile, for the single β defect the difference between the rescaled pressures calculated in the 8- and 16-atoms cells is larger, indicating that in this case a unit cell of at least 16 atoms (larger than previous studies[9,23]) is necessary for full local relaxation, again in agreement with the corresponding tabulated $E_c^{V_{\mathrm{Ge}}}$ values.

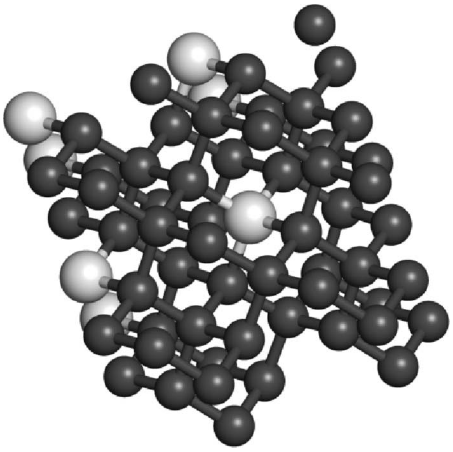

FIG. 1. α-Sn (substitutional) defects in Ge lattice. (Ge15Sn1).

In Fig. 1 we show the substitutional α-Sn defect Ge15Sn1, with a Sn atom at the center of a 16-site cell. In Fig. 2, we depict the nonsubstitutional β-Sn defect with a Sn atom at the center of a divacancy in a 16-site cell of the Ge lattice (denoted Ge14Sn1_β case), while Ge14Sn$2_\parallel$ labels the above mentioned pair defect, now placed in a 16-site Ge cell (see Fig. 3). All figures included in this section exhibit the atoms in the fully relaxed configuration obtained for each cell.

For 16-site cells we have also studied the effect of agglomeration of Sn: Ge11Sn5 corresponds to five

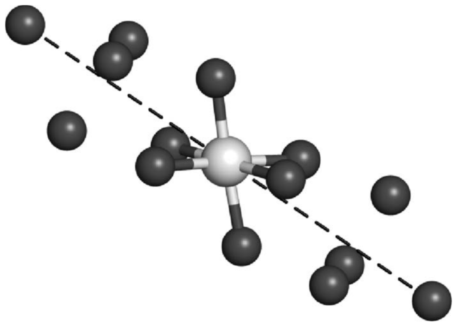

FIG. 2. β-Sn defect in Ge lattice: 16-site supercell shown. (Ge14Sn1_β).

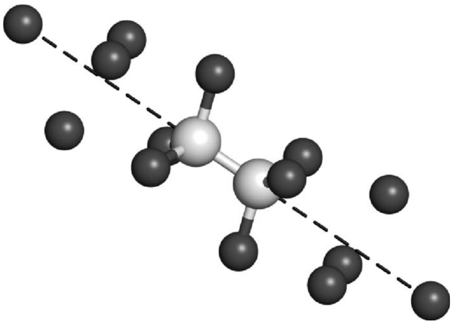

FIG. 3. Sn-pair defect in Ge lattice: 16-site supercell shown. (Ge14Sn$2_{\parallel}$)

substitutional-Sn atoms at the center of a 16-site cell; Ge11Sn4_a denotes the previous configuration with the central Sn atom removed, such that a vacancy surrounded by four Sn atoms occupies the center of the 16-site Ge-lattice cell, while Ge11Sn4_b refers to the same cell containing in its center four Sn atoms plus a vacancy now being placed at one of the nearest-neighbor sites of the cell center. We have also studied two 64-site cells, shown in Figs. 4 and 5, containing, respectively, a 6-Sn cluster-defect with a central divacancy (Ge56Sn6), and a β defect surrounded by six Sn atoms (Ge56Sn$7_{\beta'}$), always in the Ge lattice.

The last row of Table I refers to GeSn, the $x=0.5$ zincblende structure, which should be strain free. Notice that the pressure shown in last row of Table I was calculated relative to the bulk-Ge cell volume [Eq. (2)], instead of relative to the zincblende cell volume.

Our *ab initio* electronic calculations, performed in supercells larger than in previous studies[8,9,23] and with various different local defects, among other facts reveal that:

(i) cubic octahedral symmetry is favored in clusters with few Sn atoms, as can be seen in the fully relaxed configurations of Figs. 2, 4, and 5.

(ii) electronic energy per atom is not much increased by accumulating Sn clusters;

(iii) from the tabulated pressures notice that, as expected, substitutional α-Sn and nonsubstitutional β-Sn single-atom defects do, in fact, create opposite elastic fields: this leads to an effective attraction between them, such that if they do merge elastic energy is released and the small cluster relaxes to cubic symmetry;

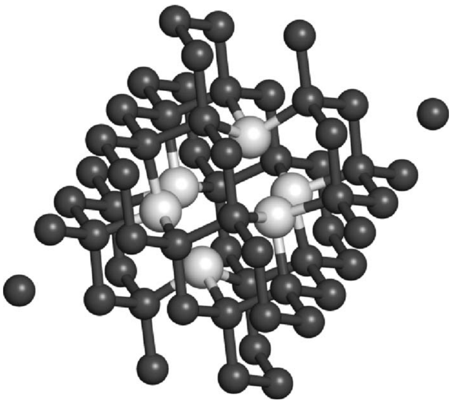

FIG. 4. 6-Sn cluster-defect with a central divacancy in Ge lattice: 64-site supercell shown. (Ge56Sn6).

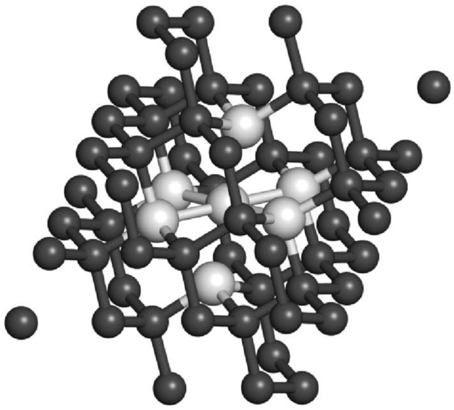

FIG. 5. 7-Sn cluster-defect (β defect surrounded by 6 Sn atoms) in Ge lattice: 64-site supercell shown. (Ge56Sn$7_{\beta'}$).

(iv) building up a local pressure in the lattice is not necessarily correlated with the electronic energy of the cluster. This agrees with former ideas about the existence of two independent difficulties for the formation of homogeneous alloys, namely, the large size difference between Ge and Sn atoms with a 15% lattice mismatch, and the d bands which make gray tin unstable at room temperature;[10,12]

(v) the energy of two α-Sn defects increases when they are closer: indicating it would be difficult to form a homogeneous high concentration totally substitutional alloy (due to the electronic energy cost). If, as generally mentioned before, strain was the only or main factor jeopardizing formation: $x=0.5$ zincblende (GeSn) should be easy to form, which is not the case.

B. Statistical mean-field approach

We used the valuable information from our electronic calculations of Sec. III A, to try to understand and predict the behavior of the alloy as a function of the Sn concentration (x). Taking advantage of the fact that both experiments and calculations indicate a favorable substitutional incorporation of Sn in the Ge matrix for low concentrations, we could model the statistical behavior of the mixture during annealing to attain thermodynamical equilibrium by a stochastic approach. At low x, defects containing only one Sn atom are relevant. Imagine a tetrahedral cage of Ge atoms in which the central four-coordinated site could be occupied by either Ge or Sn, the former representing the perfect Ge lattice (T_{Ge}) while the latter represents an α-Sn defect in Ge (T_α). By substitution of only one Sn atom in any of the corners of the cage, one gets the sixfold coordinated Sn-pair defect studied in previous section. This sixfold cage, which is the environment of a divacancy, could also be occupied by a single central Sn atom, giving the nonsubstitutional β-Sn defect studied Sec. III A (T_β). The α-Sn defect can be transformed by substitution of a single atom into the pair defect, which becomes important only for larger x. To keep the treatment to first order in x, we approximate the pair defect by two separate α-Sn defects, based on the fact that the numerical calculations of Sec. III A indicate that the energy of the pair-defect $E_{\parallel}$ is quite similar to twice the energy of one α-Sn defect, E_{α}. However, this energy difference will be taken into account below, when needed in the treatment.

To first order in x, there are only these three local configurations: $T_i(i=\alpha,\beta,\mathrm{Ge})$, which form a complete closed set, in the sense that one can transform one into the other without leaving the set by substitution of a single atom. This allows one to formulate a dynamical process, representing the formation of the infinite solid by a large number of such one-step transformations encoded in a stochastic matrix (which we will denote by **S**).[29,30] The elements of **S** can be considered as the probabilities $p_{a,b}$ of obtaining configuration b starting from configuration a, and must contain all the physical information available. Concretely, writing a one-step transformation as

$$\mathbf{S}\vec{v}_0=\vec{v}_1, \tag{3}$$

where $\vec{v}_0$ is a vector whose three components represent the initial concentrations of each of the three configurations T_i, therefore the sum of its three components equals one [i.e., $\mathrm{norm}_1(\vec{v}_0)=1$]. In general, the final vector $\vec{v}_1$ is different but its norm_1 should be conserved. This is guaranteed by normalizing the columns of matrix **S** to one, so that **S** becomes a stochastic matrix. A well-known property of stochastic matrices is that one of their eigenvalues λ_1 is equal to 1 while all others have magnitudes which are less than 1 ($|\lambda_i|<1$). After repeating the transformation n times, the transformed vector can be expressed in terms of the eigenvalues and eigenvectors $\hat{e}_i$ of the stochastic matrix **S** as,

$$\mathbf{S}^n\vec{v}_0=\sum_{i=1}^{n}\lambda_i^n a_i\hat{e}_i, \tag{4}$$

where a_i are the components of $\vec{v}_0$ in the eigenvector basis. If $n\to\infty$, the only surviving element of the summation above is

$$\mathbf{S}^n\vec{v}_0\sim(\lambda_1)^n a_1\hat{e}_1=\lambda_1 a_1\hat{e}_1=a_1\hat{e}_1. \tag{5}$$

Taking into account that $\mathrm{norm}_1(\vec{v}_0)=1=\mathrm{norm}_1(\hat{e}_1)$, and that **S** is a stochastic transformation, we immediately obtain: $a_1=1$. Therefore, the elements of $\hat{e}_1$ should be considered as the concentrations of the final configurations in the macroscopic system. For any arbitrary initial concentrations, i.e., for any $\vec{v}_0$, under homogeneous formation conditions, one attains the fixed point,

$$\hat{e}_1=(x-y,y,1-x), \tag{6}$$

where y is the concentration of β defects in the sample (and $x-y$ denotes the concentration of α defects).

The transition probabilities $p_{a,b}=P_{(a,b)}/N_{a,b}$ ($N_{a,b}$ are the required normalization factors) are composed of three parts. A first factor is the conditional probability of obtaining configuration b, starting from configuration a, that is $x_a x_b$. The second factor is a number counting all the possibilities of arranging the chemical bonds without changing the final results of the transition, and it could be interpreted as a sort of local configurational entropy. Finally, the energy barriers to perform the transition should be considered. Although the exact physical meaning of these barriers is not clear,[30] we assume that they should be proportional to the differences in the calculated energies between the local configurations involved in the transition. Even though this assumption is a simplification, we show later that the predictions of our model do not change much when using alternative definitions for the energy barriers. If the time scale for a chemical bond to reach thermal equilibrium is much smaller than the time it takes for the whole solid to equilibrate, then the third part can be written as a Boltzmann factor containing the temperature of the bath. In our case, we thus have

$$P_{\alpha\text{-Ge}}=(1-x)(x-y)4\,!\,e^{-E_{\alpha}/(k_BT)},$$

$$P_{\beta\text{-Ge}}=(1-x)y6\,!\,e^{-E_{\beta}/(k_BT)},$$

$$P_{\text{Ge-Ge}}=(1-x)^2 4\,!\,e^{-E_{\text{Ge}}/(k_BT)}. \tag{7}$$

We shall consider the remaining transition probabilities to be zero, since they are second order in y, except for the transition between two neighboring α configurations described by

$$P_{\alpha-\alpha}=(x-y)^2 4^2 3^2 e^{-(E_{\parallel}-E_{\alpha})/(k_BT)}, \tag{8}$$

due to the energy considerations which were mentioned above. Observe that the energy barrier is only the difference between the pair defect and the α defect, since only one step is needed to form it from the initial α configuration.

Summarizing, the stochastic matrix **S** takes the following form:

$$\mathbf{S}=\begin{pmatrix} A & 0 & B \\ 0 & 0 & C \\ (1-A) & 1 & (1-B-C) \end{pmatrix}, \tag{9}$$

where

$$A=\frac{P_{\alpha-\alpha}}{P_{\alpha-\alpha}+P_{\alpha\text{-Ge}}},$$

$$B=\frac{P_{\alpha\text{-Ge}}}{P_{\alpha\text{-Ge}}+P_{\beta\text{-Ge}}+P_{\text{Ge-Ge}}},$$

$$C=\frac{P_{\beta\text{-Ge}}}{P_{\alpha\text{-Ge}}+P_{\beta\text{-Ge}}+P_{\text{Ge-Ge}}}. \tag{10}$$

Notice that, due to the normalization condition, only three independent energies appear in the problem, as can be verified by, respectively, dividing numerator and denominator of A, B and C by $P_{\text{Ge-Ge}}$. Thus, only the three relative energies of each defect configuration with respect to the Ge lattice ($\tilde{E}_{\mu}\equiv E_{\mu}-E_{\text{Ge}}$) will appear, which are precisely the energies of the local defects calculated numerically in Sec. III A.

The eigenvector of **S** with eigenvalue 1 is

$$\hat{e}_1=(x_{\alpha},x_{\beta},x_{\text{Ge}}), \tag{11}$$

where

$$x_{\alpha}=\frac{B}{1-A}x_{\text{Ge}},$$

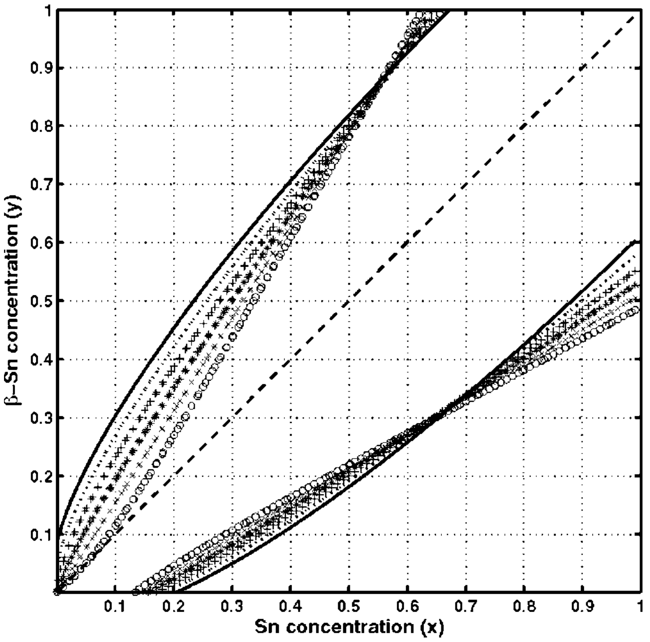

FIG. 6. Concentration of β-Sn defects as a function Sn concentration in a $Ge_{1-x}Sn_x$ alloy, at different temperatures. Full line: $T=16$; 39 (dotted); 62 (plus signs); 85 (asterisks); 108 (crosses); 131 °C (circles).

$$x_\beta = C x_{\mathrm{Ge}},$$

$$x_{\mathrm{Ge}} = \frac{1-A}{(1-A)(1+C)+B}, \qquad (12)$$

which due to the homogeneity condition should be identical to Eq. (6).

Therefore, at a fixed temperature (T) one can obtain the concentration of β-Sn defects by finding the zeros of the function,

$$f(x,y) = \frac{1-A}{(1-A)(1+C)+B} - (1-x), \qquad (13)$$

which we do numerically. The needed values of the energies are taken from Table I and are $\tilde{E}_\alpha=0.018$ eV, $\tilde{E}_\beta=0.120$ eV, and $\tilde{E}_\parallel=0.041$ eV.

In Fig. 6 we depict the zeros of $f(x,y)$ obtained for six different temperatures. Notice that the only physically meaningful solutions are the ones below the $y=x$ line (since the β-defect concentration y cannot be larger than the total Sn concentration present, x). Observe that at room temperature there are no β defects present for concentrations $x<0.2$, meaning that the alloy is perfectly substitutional (only α-Sn defects present). Therefore, a continuous shift of the electronic properties is to be expected and could be accurately modeled by a simple VCA approximation, as previously noted and measured[7,10] and we will further discuss in Sec. III C. For larger Sn concentration, $x>0.2$, one finds that a nonzero concentration of β-Sn defects appear, which would introduce electronic traps in the gap of the alloy. A monotonous increase in the number of β defects follows, as more Sn is incorporated to the Ge lattice.

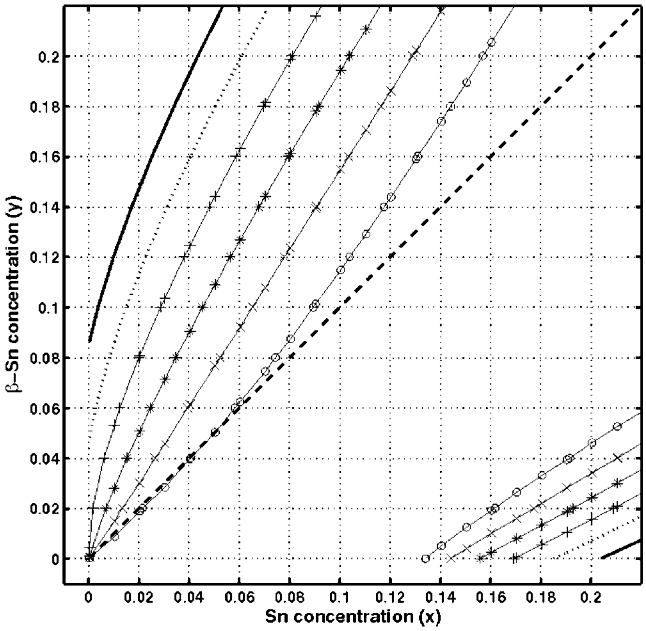

FIG. 7. Amplification of the low-concentration region of Fig. 6. Full line: $T=16$; 39 (dotted); 62 (plus signs); 85 (asterisks); 108 (crosses); 131 °C (circles).

Furthermore, our simple model predicts that as the temperature of formation of the solid is increased the β defects start to appear at lower Sn concentrations, as expected because the increase in thermal energy favors the overcoming of all energy barriers. This fact provides an explanation for the findings of $Ge_{1-x}Sn_x$ alloy preparation by chemical vapor deposition (CVD),[10] where it has been observed that more substitutional Sn could be incorporated if the substrate temperature is lowered. This is also known to happen in amorphous $Ge_{1-x}Sn_x$ alloys.[17]

In Fig. 7 we show an amplification of the low-concentration results, where the above discussed dependence on temperature is clearly seen. Also, notice that for high enough temperature the nonphysical roots start to cross the $x=y$ line, meaning that β defects can be formed at any Sn concentration. This is expected to happen because disposing of large amounts of thermal energy allows the significant creation of more complex defects than those considered in this simple approximation. We think that there is not much to gain by increasing the complexity of the present model, since the larger the defect space considered, the less reliable are the local energies calculated.

Finally, in Fig. 8 we show the effect of using the alternative definition for the defect energy obtained by partial relaxation, fixing the cell volume at the bulk-Ge value ($E_d^{V_{\mathrm{Ge}}}$). As expected from the differences in respective energies stated in Table I, which show a relatively lower increase for the β-defect energy than for the α or pair-defect cases, fixing the cell volume leads to β defects appearing at slightly lower Sn concentration values. The comparison of results using the alternative defect energy definitions reveals that the main

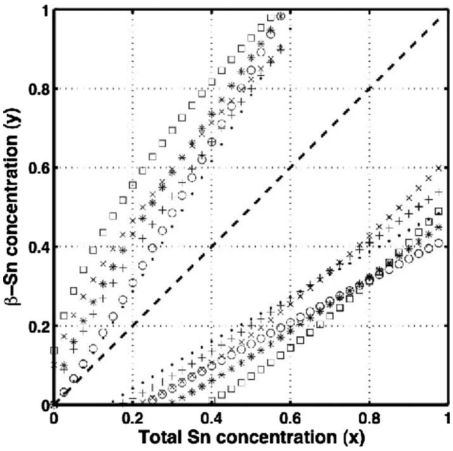

FIG. 8. Comparison of use of alternative defect energy definitions: relaxed vs fixed at V_{Ge} cell volumes, on the concentration of β-Sn defects as a function of total Sn concentration. Using E_d, at: $T=18$ (squares); 79 (asterisks); 134 °C (circles). Using $E_d^{V_{\mathrm{Ge}}}$, at the same temperatures: 18 (crosses); 79 (plus signs); 134 °C (dots).

effect of using the partial relaxation is a general shift (reduction) in the "effective" energy barriers in the Boltzmann factors of Eqs. (7) and (8): thus being analogous to a rescaling of the temperature.

C. Electronic structure studies

1. Supercell calculations

The *ab initio* local defect calculations presented in Sec. III A also yield the density of states and energy bands of perfectly ordered periodic crystals formed by those supercells. As an illustration we show in Fig. 9 the densities of states (DOS) of three characteristic crystals, namely, the pure Ge and Sn ones, and the zinc-blende-type GeSn, previously studied in Ref. 31.

It can be noticed in Fig. 9 that the Ge bands are slightly wider than the Sn ones, and that the density of states of GeSn at the Fermi level lies between the higher value for Sn and the very small value obtained for Ge, as one would expect. Notice that the pure Ge DOS does not have a gap at the Fermi level, which is not a surprise due to inaccuracies at small energies around the Fermi level of the approach GGA-WIEN2K. Another peculiar thing is the fact that deep down the valence band (around 8 eV), both pure systems present a single Van Hove singularity with zero DOS corresponding to degeneracy of the bands at the X point of the first Brillouin zone of the fcc diamond structure. This degeneracy is due to the inversion symmetry, which is lacking in the zincblende structure. The wide gap in the density of states around those energies exhibited in zinc-blende GeSn is due to the removal of this degeneracy.[31] Of course, such features due to symmetry breaking are not expected in the real crystalline alloys since perfect order is not realized. All this can be seen more clearly in Fig. 10, where the electronic bands from the two-atom cell are shown. Observe that the lowest conduction band crosses the Fermi level at point L.

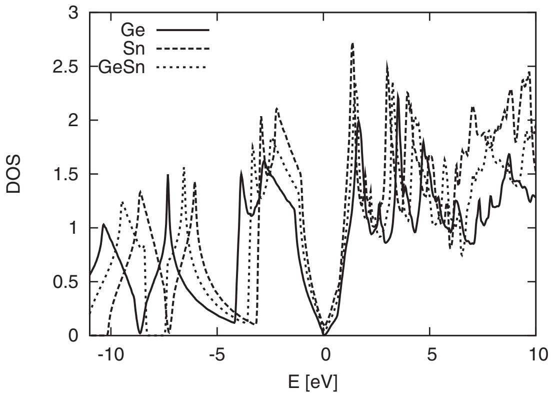

FIG. 9. *Ab initio* (WIEN-2K) calculated DOS with 16-atom supercells.

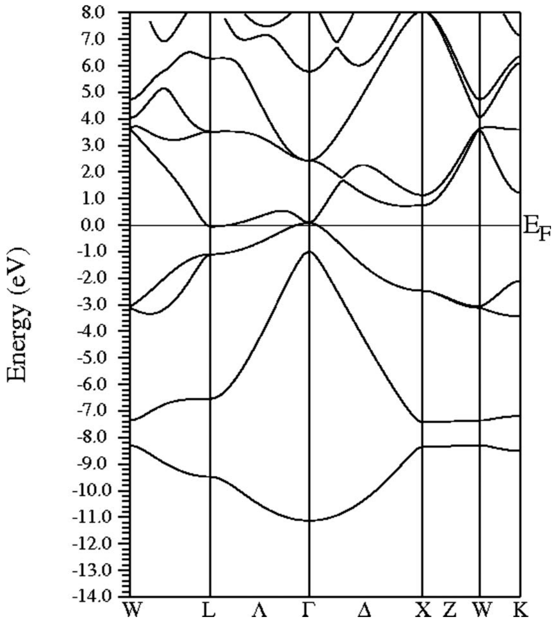

FIG. 10. *Ab initio* (WIEN-2K) calculated bands with 2-atom cells for GeSn.

2. Tight binding+VCA

Tight-binding (TB) calculations for electronic band structures are very useful because, besides their simplicity, it is possible to incorporate many features by suitably choosing the TB parameters. These methods applied to Ge proved not to be straightforward, since a naive calculation considering sp^3 orbitals is unable to reproduce essential features like the indirect band gap and the bandwidths. This is due to the mixing of d electrons in the conduction bands of Ge, which for Si or C are not important, while for Sn and Pb are responsible for their metallic behavior. The role of d electrons could be mimicked by introducing a pseudo-orbital (s^*) without increasing the size of the TB Hamiltonian. Finer properties, such as the exciton spectrum of Ge cannot be explained without introducing spin-orbit interactions.

In 1987, Jenkins and Dow[7] presented a complete TB model for the $\mathrm{Ge}_{1-x}\mathrm{Sn}_x$ alloy, including spin-orbit, s^*, and second-neighbor interactions. They examined several properties by using a simple virtual-crystal approximation[19] de-

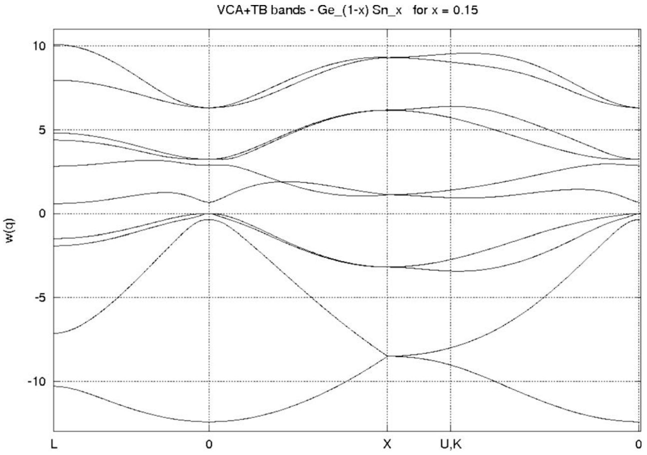

FIG. 11. TB+VCA calculated bands as in Ref. 7 for $Ge_{1-x}Sn_x$ at $x=0.15$.

scription of the alloy. Their results are in very good agreement with experiments for low concentrations, in particular they predict the indirect-to-direct-gap transition to occur at $x \approx 0.15$. For the sake of completeness and to facilitate comparison with the low-concentration regime, we have reproduced their TB+VCA calculations, and in Fig. 11 we depict the electronic bands precisely at this critical concentration. Notice that the optical gap is the same at the center of the first Brillouin zone and at point L.[7]

The dependence of electronic properties as a function of concentration continues smoothly in this approximation, contrary to the experimental facts. To illustrate this, in Fig. 12 we plot the bands at 50% concentration, where a small energy gap at the Fermi level is still present. Spectroscopic ellipsometry and photoreflectance experiments[16] found that there is a strong bowing tendency, i.e., nonlinear behavior of this gap with concentration, that would close the gap at a much lower value: $x \approx 0.37$. As one expects for the alloy, no degeneracy is removed at point X, because it does not introduce spurious order such as the zinc-blende band structure of Fig. 10.

In summary, these TB+VCA calculations can be trusted only at low concentrations, where they provide a valuable tool to interpret experiments.

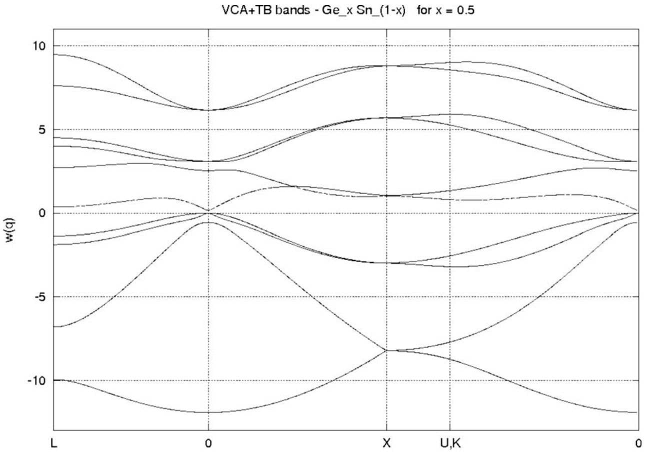

FIG. 12. TB+VCA calculated bands as in Ref. 7 for $Ge_{1-x}Sn_x$ at $x=0.5$.

3. Coherent potential approximation

In many random alloys, the coherent-potential approximation[20] for the treatment of substitutional disorder leads to an improved description of the electronic structure, overcoming some limitations of the VCA discussed in Sec. III C 2. CPA has been applied successfully to many semiconductors,[21] and in particular to $Ge_{1-x}Si_x$ alloys[22] where it predicts moderate bowing in the optical transition energies. Concerning $Ge_{1-x}Sn_x$, special supercell calculations have been performed to mimic the alloy by averaging over selected structures.[23,32] They predict a large and compositional-dependent direct-gap bowing, in agreement with experimental reports.[16]

CPA electronic structure studies of the $Ge_{1-x}Sn_x$ alloy were lacking, up to now. This has prompted us to undertake them, in order to complete the information available for these compounds. Also, since the approximation is known to give excellent predictions in many substitutional semiconductor alloys,[21,22] a failure to describe the experimental findings in $Ge_{1-x}Sn_x$ needs careful consideration but could provide an insight into material-specific characteristics. Here, limitations of a traditional CPA approach might be expected to arise in connection with the size and chemical mismatch present between the constituents of the substitutional alloy, but they could also result from the presence of nonsubstitutional disorder in the system, as we discuss below.

We decided to use a more advanced implementation of the CPA, combining it with the power of *ab initio* band-structure description, which allows us to take into account material-specific characteristics of the two constituent species of the alloy. Concretely, we used the FPLO-5 numerical code developed by the IFW-Dresden group.[33,34] This package is a full-potential local-orbital minimum-basis code, combining *ab initio* local spin-density approximation (LSDA) band-structure treatment[33] with single-site CPA routines for substitutional disorder[34] (specifically, it employs the Blackmann-Esterling-Berk single site-CPA extension for combined diagonal and nondiagonal disorders[35]). Moreover, to improve our CPA description, considering the size mismatch between Ge and Sn, we took into account the structural changes undergone as a function of Sn concentration as described below. In the following, we report results of our CPA calculations for the $Ge_{1-x}Sn_x$ alloy using the FPLO-5 code.

In Fig. 13 we show the FPLO+CPA total density of states for $Ge_{1-x}Sn_x$ as a function of energy, at different substitutional-Sn concentrations: $x=0.0, 0.062, 0.125, 0.25, 0.5$. Notice that a smooth behavior as a function of concentration is obtained, with changes in the bandwidth, and a progressive filling of the gap at the Fermi level with Sn concentration, as one would expect. Experiments in $Ge_{1-x}Sn_x$ alloys[36] have indicated that the direct energy band gap decreases primarily through an increase in alloy concentration (and applied coherency strain mainly reduces the valence-band DOS, instead of the magnitude of the gap).

Our results were obtained adjusting the input lattice parameters at each alloy concentration using our respective WIEN-2K obtained structural data (Table I). If, as it is usual in CPA, one uses the fixed lattice parameter corresponding to the perfect ($x=0$) lattice at all concentrations, one finds that

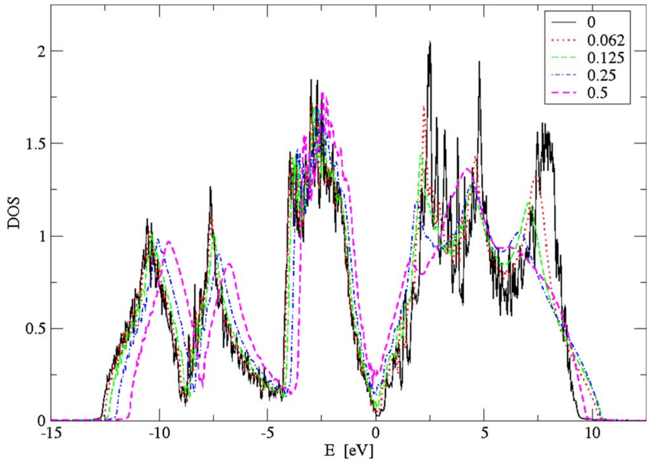

FIG. 13. (Color online) CPA for $Ge_{1-x}Sn_x$, via FPLO-5 code: total density of states for the α-Sn concentrations indicated inside plot. Lattice parameters from respective WIEN-2K obtained structural data.

the trends with concentration are much smaller, if observable. For instance, the resulting valence band obtained is almost unchanged by concentration increases of up to 25%, thus not reflecting the effect of the difference of bandwidths (and shapes) of the two alloy components. In this sense we have found that some improvement is gained by supplementing this effective-field method with information on the structural changes undergone by the alloy as a function of concentration, considering that we found limitations of the traditional CPA description for $Ge_{1-x}Sn_x$ even at relatively low concentrations.

To better convey the information obtained by the FPLO +CPA approach, in Fig. 14 we show the CPA results at $x=0.125$, namely, the total density of states as well as the orbital-resolved partial densities of states. At this low Sn concentration, the total DOS follows closely the Ge-host one.

Increasing concentration to $x=0.25$, in Fig. 15 we show the total DOS as well as the orbital-resolved partial DOS: here the most relevant ones correspond to s orbitals (given by the 4s orbitals in Ge, and the 5s ones in Sn) and p orbitals (4p of Ge, and 5p of Sn) while, for clarity, the relatively smaller d components are not shown. Our results show good agreement with the valence-band s and p partial DOS obtained by a previous LMTO Green's function study.[37] Basically, the spectral weight of p orbitals strongly dominates around the Fermi level, while the s orbitals are the most relevant at lower energies, for both species.

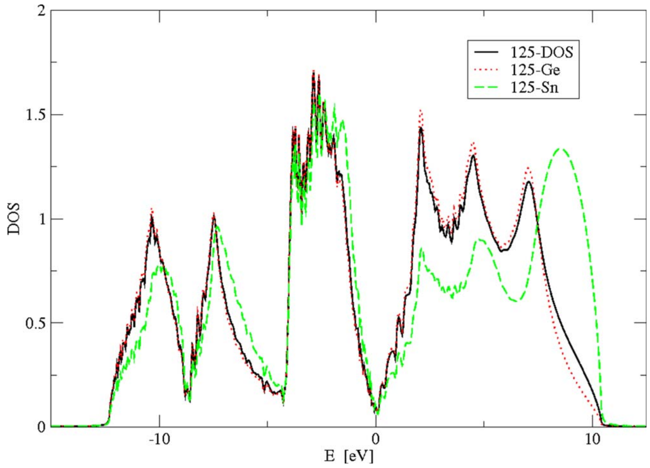

FIG. 14. (Color online) CPA results for $Ge_{0.875}Sn_{0.125}$, via FPLO-5: total and partial (species resolved) DOS for each alloy component, as a function of energy.

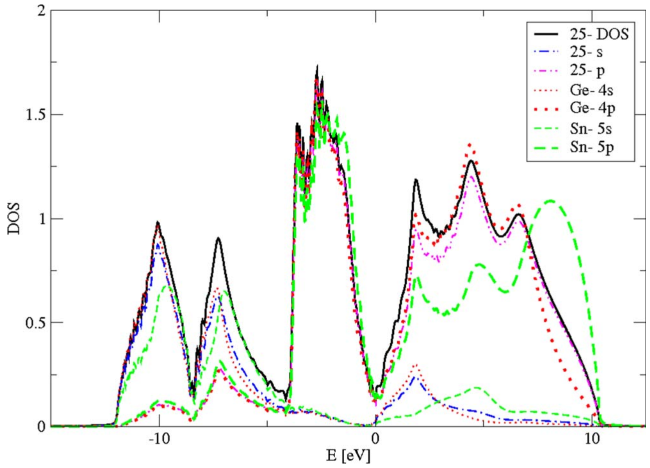

FIG. 15. (Color online) CPA results for $Ge_{0.75}Sn_{0.25}$, via FPLO-5: total density of states, orbital and orbital+species resolved main DOS contributions, as functions of energy (references in plot).

Finally, in Fig. 16 we exhibit an example of the problems encountered by the CPA approach used, based on the assumption that only substitutional α-Sn impurities are present, which cannot be overcome even by the inclusion of *ab initio* material-specific features and by taking into account lattice parameter changes as a function of Sn concentration to consider the size mismatch of the constituents of the alloy. Here the $x=1$ density of states is shown, in addition to the $x=0,0.5$ ones, showing that the smooth trend with Sn concentration of Fig. 13, consisting of the filling of the gap at the Fermi level, is not valid at larger concentrations ($x\geq 0.5$).

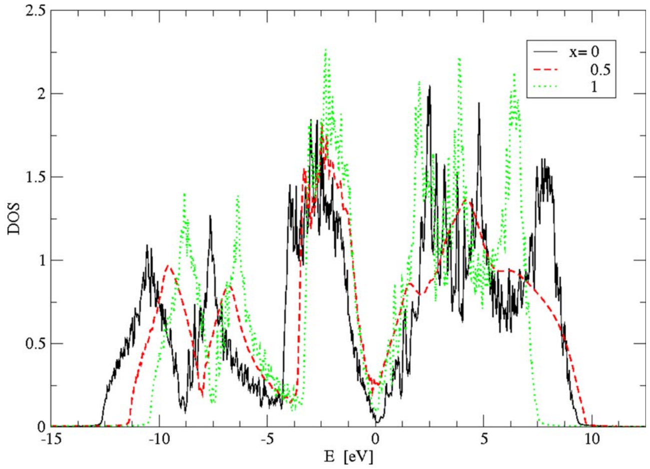

FIG. 16. (Color online) CPA via FPLO-5 calculated DOS for Ge, Sn and $Ge_{0.5}Sn_{0.5}$.

Contrary to expectations, the DOS at the Fermi level for pure Sn is not the largest obtained for the alloy series.

We believe that a complete and consistent treatment of the electronic structure should include an evaluation of the effects of nonsubstitutional Sn, an ingredient which might improve the description presented above. The need to include nonsubstitutional β-Sn defects is called for by the experimental evidence of their existence in nonhomogeneous Ge-Sn compounds, and by the results of our study for the incorporation mechanisms of Sn into the Ge matrix through our detailed *ab initio* defect study and statistical model.

IV. CONCLUSIONS

We have proposed a mechanism to understand the peculiar properties of $Ge_{1-x}Sn_x$ alloys. The main assumption is the existence of the β-Sn defect, occupying a divacancy in the Ge host, which imposes a severe strain in the lattice opposite to the one caused by the α-Sn substitutional defect. The other feature of the β defect is that it causes a sixfold octahedral coordination on the Sn atom, favoring the nucleation of white tin inclusions which eventually segregate. The existence of such nonsubstitutional-Sn defect is an observed experimental fact in nonhomogeneous samples.[17,18]

We demonstrate the plausibility of this assumption for $Ge_{1-x}Sn_x$ alloys by performing *ab initio* electronic calculations in supercells containing different local defects. We started from the single atom α and β defects, and then increased the number of Sn atoms, in order to estimate: the electronic energy, the relaxed configuration around the defects, and the pressure caused by them. These studies suggest that the cubic octahedral symmetry is favored in clusters containing few Sn atoms, and that the electronic energy per atom is not very much increased by accumulating clusters of Sn. The calculated pressures indicate that the large positive elastic field around these large defects may be released by the aggregation of β defects, which have an opposite elastic field. We have observed that building up a local pressure in the lattice is not necessarily correlated with the electronic energy of the cluster. This is in agreement with former ideas[10,31] that there are two independent reasons to account for the difficulties to form homogeneous $Ge_{1-x}Sn_x$ alloys, namely, the electronic d bands which make gray α-Sn unstable at room temperature and the large difference in the size of the atoms. We have also observed that the energy of two α defects increases when they are closer together, also indicating that it would be very difficult to obtain a homogeneous alloy formed only by α defects since their mean-distance would be smaller than a unit cell. Notice that if strain was the only factor jeopardizing formation, the $x=0.5$ zincblende compound should be easy to form since it would be strain-free, but this is not the case.

The knowledge gained by the local defect studies provided the basic ingredients to formulate a simple statistical model to investigate the relative concentration of α and β defects in thermal equilibrium as a function of the total Sn concentration, x. The model focuses on the dynamical evolution of few local configurations by using a stochastic matrix containing all the statistical information to calculate the transition between one configuration to another. The results show that, at room temperature, there are no β defects present for $x<0.2$. Thus, our model supports the experimental finding that, at concentrations below 20%, Sn only enters substitutionally with a local tetrahedral environment. We find that the number of β defects at a given concentration increases with temperature. We also found that the concentration at which β defects start appearing decreases at larger temperatures. This suggests that one could obtain homogeneous alloys with higher Sn content if one decreases the temperature of the thermal bath. This would mean, in the case of epitaxial growing by CVD or other techniques, that lowering the temperature of the substrate on which the alloy is grown favors the formation of homogeneous alloys at higher Sn concentrations. This agrees with the experimental findings.[10] In particular, we predict that $x=0.5$ homogeneous alloys would be possible to form at temperatures below -90 °C.

In the last part of our work, we have tried to gain more insight into the problem by using effective-field methods in order to investigate the lower concentration region in more detail. There, we found that TB+VCA, while providing a good description of the substitutional-dominated regime, fails to predict the closing of the electronic gap at $x=0.37$ seen in experiments. Furthermore, more sophisticated mean-field techniques as the CPA (even using a combined *ab initio* realistic band structure with the single-site substitutional CPA), does not provide much improvement. If one tries to take into account the size mismatch by supplementing this FPLO+CPA approach with the concentration dependence of the lattice parameter obtained from our *ab initio* local defect calculations (in agreement with experiments), a slight improvement of the results is obtained though problems still persist.

Based on the experimental evidence for existence of nonsubstitutional β-Sn defects in nonhomogeneous Ge-Sn compounds, and the results of the present work for the Sn incorporation mechanisms into Ge obtained by our detailed *ab initio* defect study and the statistical model, we believe that the effects of nonsubstitutional Sn need to be assessed and taken into account for any complete description of $Ge_{1-x}Sn_x$ alloys. In particular, an extension of the CPA (Ref. 38) able to take into account more complex Sn defects, as the nonsubstitutional β defect, would certainly be extremely useful for a complete and consistent description of the electronic properties of these fascinating and useful alloys, and to study their effect on the large bowing of the direct band gap and the indirect to direct-gap crossover.[16,23,32,39,40] Research along these lines is currently in progress.

ACKNOWLEDGMENTS

We thank M. Richter, K. Koepernik, H. Eschrig, and the FPLO team, for the support and help to run their FPLO-CPA code, and for useful discussions; also J. Menendez, P. Fulde, and B. Bouhafs for useful references and discussions. We are specially grateful to Rubén Weht for his help in running additional FPLO-CPA cases and for his careful reading of the paper. C.I.V. and J.D.F. are Investigadores Científicos of CONICET (Argentina). C.I.V. acknowledges support from CONICET and ANPCyT (Grants No. PIP'5342 and No. PICT'38357); from I.C.T.P., Trieste, Italy, as *Regular Associate*; E.Peltzer and organizers of the 6th-FPLO Workshop (La Plata, Argentina, 2007), and the hospitality of Theoretical Physics and Worcester College, University of Oxford, U.K., where parts of this work were completed. R.A.B. thanks Centro Atómico Bariloche and CMB Mathematical Institute, University of Oxford, for hospitality; sabbatical grants from DGAPA (UNAM) and CONACyT are fully acknowledged.

---

[1] R. J. Temkin, Solid State Commun. **11**, 1591 (1972).
[2] C. H. L. Goodman, IEE Proc., Part I: Solid-State Electron Devices **129**, 189 (1982).
[3] S. Oguz, W. Paul, T. F. Deutsch, B. Y. Tsaur, and D. V. Murphy, Appl. Phys. Lett. **43**, 848 (1983).
[4] T. P. Pearsall, J. Bevk, L. C. Feldman, J. M. Bonar, J. P. Mannaerts, and A. Ourmazd, Phys. Rev. Lett. **58**, 729 (1987).
[5] See e.g., Peter Y. Yu and Manuel Cardona, *Fundamentals of Semiconductors: Physics and Materials Properties*, 3rd ed. (Springer-Verlag, Berlin, 2003).
[6] S. Groves and W. Paul, Phys. Rev. Lett. **11**, 194 (1963).
[7] D. W. Jenkins and John D. Dow, Phys. Rev. B **36**, 7994 (1987).
[8] K. A. Mäder, A. Baldereschi, and H. von Känel, Solid State Commun. **69**, 1123 (1989).
[9] G. He and H. A. Atwater, Phys. Rev. Lett. **79**, 1937 (1997).
[10] M. Bauer, J. Taraci, J. Tolle, A. V. G. Chismeshya, S. Zollner, D. J. Smith, J. Menendez, Changwu Hu, and J. Kouvetakis, Appl. Phys. Lett. **81**, 2992 (2002).
[11] M. R. Bauer, J. Tolle, C. Bungay, A. V. G. Chismeshya, D. J. Smith, J. Menendez, and J. Kouvetakis, Solid State Commun. **127**, 355 (2003).
[12] H. Pérez Ladrón de Guevara, A. G. Rodriguez, H. Navarro-Contreras, and M. A. Vidal, Appl. Phys. Lett. **84**, 4532 (2004).
[13] R. Ragan, J. E. Guyer, E. Meserole, M. S. Goorsky, and H. A. Atwater, Phys. Rev. B **73**, 235303 (2006).
[14] J. D. Sau and M. L. Cohen, Phys. Rev. B **75**, 045208 (2007).
[15] S. F. Li, M. R. Bauer, J. Menendez, and J. Kouvetakis, Appl. Phys. Lett. **84**, 867 (2004).
[16] V. R. D'Costa,C. S. Cook, A. G. Birdwell, C. L. Littler, M. Canonico, S. Zollner, J. Kouvetakis, and J. Menendez, Phys. Rev. B **73**, 125207 (2006).
[17] I. Chambouleyron, F. Marques, P. H. Dionisio, I. J. R. Baumvol, and R. A. Barrio, J. Appl. Phys. **66**, 2083 (1989).
[18] P. Boolchand and C. C. Koch, J. Mater. Res. **7**, 2876 (1992).
[19] L. Nordheim, Ann. Phys. **9**, 607 (1931).
[20] P. Soven, Phys. Rev. **156**, 809 (1967).
[21] M. Jaros, Rep. Prog. Phys. **48**, 1091 (1985).
[22] D. Stroud and H. Ehrenreich, Phys. Rev. B **2**, 3197 (1970); S. Krishnamurthy, A. Sher, and A. B. Chen, *ibid.* **33**, 1026 (1986).
[23] Y. Chibane, B. Bouhafs, and M. Ferhat, Phys. Status Solidi B **240**, 116 (2003).
[24] P. Blaha, K. Schwarz, G. K. H. Madsen, D. Kvasnicka, and J. Luitz, *WIEN2k, An Augmented Plane Wave+Local Orbitals Program for Calculating Crystal Properties* (Karlheinz Schwarz, T.U. Wien, Austria, 2001).
[25] K. Schwarz, P. Blaha, and G. K. H. Madsen, Comput. Phys. Commun. **147**, 71 (2002).
[26] K. Schwarz and P. Blaha, Comput. Mater. Sci. **28**, 259 (2003).
[27] J. P. Perdew, S. Burke, and M. Ernzerhof, Phys. Rev. Lett. **77**, 3865 (1996).
[28] H. J. Monkhorst and J. D. Pack, Phys. Rev. B **13**, 5188 (1976).
[29] R. A. Barrio, R. Kerner, M. Micoulaut, and G. G. Naumis, J. Phys.: Condens. Matter **9**, 9219 (1997).
[30] R. Kerner, *Models of Agglomeration and Glass Transition* (Imperial College Press, London, 2006).
[31] T. Brudevoll, D. S. Citrin, N. E. Christensen, and M. Cardona, Phys. Rev. B **48**, 17128 (1993).
[32] P. Moontragoon, Z. Ikonic, and P. Harrison, Semicond. Sci. Technol. **22**, 742 (2007).
[33] K. Koepernik and H. Eschrig, Phys. Rev. B **59**, 1743 (1999); I. Opahle, K. Koepernik, and H. Eschrig, *ibid.* **60**, 14035 (1999).
[34] K. Koepernik, B. Velicky, R. Hayn, and H. Eschrig, Phys. Rev. B **55**, 5717 (1997).
[35] J. Blackman, D. Esterling, and N. Berk, Phys. Rev. B **4**, 2412 (1971); for a review of approaches to disorder see, e.g., A. Gonis, *Green Functions for Ordered and Disordered Systems* (North-Holland, Amsterdam, 1992).
[36] R. Ragan and H. A. Atwater, Appl. Phys. Lett. **77**, 3418 (2000).
[37] A. Svane, J. Phys. C **21**, 5369 (1988).
[38] C. I. Ventura and R. A. Barrio, Physica B **281-282**, 855 (2000).
[39] V. R. D'Costa, C. S. Cook, J. Menendez, J. Tolle, J. Kouvetakis, and S. Zollner, Solid State Commun. **138**, 309 (2006).
[40] K. Alberi, J. Blacksberg, L. D. Bell, S. Nikzad, K. M. Yu, O. D. Dubon, and W. Walukiewicz, Phys. Rev. B **77**, 073202 (2008).